

Spontaneous Polarization of the Neutral Interface for Valence Asymmetric Coulombic Systems

D. di Caprio*

Laboratory of Electrochemistry and Analytical Chemistry, University Paris 6, CNRS, ENSCP, Université Paris 6, B.P. 39 4, Place Jussieu, 75252 Paris Cedex 05, France

M. Holovko

Institute for Condensed Matter Physics, National Academy of Sciences, 1 Svientsitskii Str., 79011 Lviv, Ukraine

Received: September 30, 2008; Revised Manuscript Received: December 3, 2008

In this paper, we discuss the phenomenon of a spontaneous polarization of a neutral hard planar interface for valence asymmetric Coulombic systems. Within a field theoretical description, we account for the existence of nontrivial charge density and electric potential profiles. The analysis of the phenomenon shows that the effect is related to combinatorics in relation with the existence of the two independent species cations and anions. This simple and basic feature is related to the quantum mechanical properties of the system. The theoretical results are compared with numerical simulations data and are shown to be in very good agreement, which a fortiori justifies our physical interpretation.

I. Introduction

There has been recently a renewed interest in the study of the structure of the double layer. This stems from both the existence of new important domains of application as for instance those related with the nanotechnologies, microfluidics, microbatteries, and electrochemical sensors, biology and also the use of new ionic liquid solvents.^{1,2} These new domains represent a theoretical challenge as the behavior of the charged systems does not in general follow the popular predictions of the Poisson–Boltzmann approach. There can be many reasons for parting from the standard behavior. For instance, it can be related to excluded volume like packing effects at high local concentrations at the interface^{1,2} but also, in the regime of low reduced temperatures, to the existence of strong Coulomb interactions which require to account for correlations beyond mean field theories like the popular Gouy–Chapman (GC) approach. In the latter case, there has been a series of papers^{3–13} devoted to the challenging problem of the anomalous behavior of the electric capacitance.

In this paper, we investigate another type of systems which also depart from the standard GC approach. It is the case of the asymmetric in valence electrolytes. In an early paper, Torrie et al.¹⁴ have shown the existence of a polarization of the interface even at the point of zero charge (PZC) for an extended restricted primitive model of ions with different valences. This phenomenon is far from obvious and standard intuitive approximations like the GC theory are unable to describe it. In contrast to the case of asymmetric in size ions, where the smallest ion by coming closer to the interface induces a polarization of the interface, the behavior of valence asymmetric ions is rather nonintuitive. Torrie et al. have used a modified Poisson–Boltzmann approach to describe this effect which is in our opinion rather costly in its mathematical application. More recently, Henderson et al.¹⁵ have addressed the problem using standard approximations in the liquid state theory searching for simple analytic

expressions. They were able to reproduce the polarization effect for the size asymmetry but not for the valence asymmetry. From a practical point of view, the interest of studying the behavior of the PZC is that this quantity is often considered as an indication of chemical interaction of the ions with the electrode so-called “specific adsorption”. Here, by considering a hard wall, we discard the role of specific interactions and intend to propose an alternative simple physical interpretation.

The article is organized as follows. In the first section, we present the field theory formalism for valence asymmetric electrolytes and introduce the meaningful physical parameters for the system. In the following two sections III and IV, we derive respectively the expressions of the charge profile and of the electric potential across this interface at a neutral hard wall. Then, in section V, we compare the results to the exact relation given by the charge contact theorem¹⁶ and verify the consistency of our expressions. Finally, in section VI, we discuss the different profiles with respect to numerical simulations results.¹⁵

II. Field Theory for Point Ions

A. Formalism. We consider a field theoretical description of a system of point ions situated in a half-space, in contact with a hard wall. The dielectric constant $\varepsilon = \varepsilon_r \varepsilon_0$ is uniform throughout the space. As in refs 11 and 17, we introduce a field theoretical expression of the grand potential in terms of the fields $\rho_+(\mathbf{r})$ and $\rho_-(\mathbf{r})$ representing in space the density fields for cation and anion distributions, respectively

$$\Xi[\rho_{\pm}] = \int \mathcal{D}\rho_{\pm}(\mathbf{r}) \exp\{-\beta H[\rho_{\pm}]\} \quad (1)$$

where $\beta = 1/(k_B T)$ is the inverse temperature. The grand potential is then obtained as $\beta(-pV + \gamma A) = -\ln \Xi[\rho_{\pm}]$, where p is the pressure, V is the volume, γ is the surface tension, and A is the area of the electrodes. For the study of the Coulomb interactions, it is convenient to use the charge density field $q(\mathbf{r}) = z_+ \rho_+(\mathbf{r}) - z_- \rho_-(\mathbf{r})$, with z_+ , z_- the valences of cations and

* To whom correspondence should be addressed. E-mail: dung.di_caprio@upmc.fr.

anions respectively, and the total density field $s(\mathbf{r}) = \rho_+(\mathbf{r}) + \rho_-(\mathbf{r})$. The Hamiltonian as a functional of these fields is

$$\beta H[q, s] = \beta H^{\text{ent}}[q, s] + \beta H^{\text{Coul}}[q] - \int \beta \mu_s s(\mathbf{r}) d\mathbf{r} - \int \beta \mu_q q(\mathbf{r}) d\mathbf{r} \quad (2)$$

where $\mu_s = \mu_+ + \mu_-$, $\mu_q = z_+ \mu_+ - z_- \mu_-$, and μ_{\pm} are the chemical potentials of the ions. The first and last terms of the Hamiltonian account for the quantum mechanical degrees of freedom^{17,18} and the chemical potential contributions. As they do not involve the interactions, we shall then associate them and choose to call this ensemble the entropic functional term in the Hamiltonian. We emphasize that this entropic functional should not be mistaken with the thermodynamic entropy; the functional appears at the level of the Hamiltonian and it is not a thermodynamic potential. This functional is entropic in the sense that the quantum mechanics tells us to what extent we can distinguish independent states in the phase space, and this sets the familiar combinatorics which appears for instance in the $1/(N_+!N_-!)$ term in the standard statistical mechanics when we have N_+ cations and N_- anions. In our case, these properties are written in the following entropic functional in the Hamiltonian

$$\beta H^{\text{ent}}[q, s] = \int \beta \mu_s s(\mathbf{r}) d\mathbf{r} - \int \beta \mu_q q(\mathbf{r}) d\mathbf{r} - \int \frac{q(\mathbf{r}) + s(\mathbf{r})}{2} \left[\ln \left(\frac{q(\mathbf{r}) + s(\mathbf{r})}{2\bar{\rho}_+} \right) - 1 \right] d\mathbf{r} + \int \frac{s(\mathbf{r}) - q(\mathbf{r})}{2} \left[\ln \left(\frac{s(\mathbf{r}) - q(\mathbf{r})}{2\bar{\rho}_-} \right) - 1 \right] d\mathbf{r} \quad (3)$$

where $\bar{\rho}_{\pm} = \exp(-\beta \mu_{\pm})/\Lambda^3$ with Λ being the de Broglie wavelength. The second term in the Hamiltonian is the Coulombic contribution

$$\beta H^{\text{Coul}}[q] = \frac{\beta e^2}{8\pi\epsilon} \int \frac{q(\mathbf{r})q(\mathbf{r}')}{|\mathbf{r} - \mathbf{r}'|} d\mathbf{r} d\mathbf{r}' \quad (4)$$

where e is the elementary electric charge.

In order to perform the calculations we expand the Hamiltonian of eq 2 around the mean field profiles $\bar{q} = 0$ and $\bar{s} = \bar{\rho}$ which minimize the Hamiltonian in the case of the neutral hard wall,¹⁹ where $\bar{\rho} = \bar{\rho}_+ + \bar{\rho}_-$. Beyond the mean field solution, introducing $\delta s = (s - \bar{\rho})/\bar{\rho}$ and $\delta q = q/\bar{\rho}$, the Hamiltonian is

$$\beta H = \bar{\rho}V + \frac{\bar{\rho}}{2} \int \left[\delta s^2(\mathbf{r}) + \frac{\delta q^2(\mathbf{r})}{z_{\text{is}}^2} \right] d\mathbf{r} + \beta \delta H + \beta H^{\text{Coul}}[q] \quad (5)$$

where $\beta \delta H$ contains terms of the expansion of orders higher than quadratic. We introduce $z_{\text{is}} = \sqrt{(z_+ z_-)^{1/2}}$, and $z_{\text{as}} = (z_+ - z_-)/\sqrt{(z_+ z_-)^{1/2}}$. The first coefficient is related to the ionic strength as $z_+^2 \bar{\rho}_+ + z_-^2 \bar{\rho}_- = z_+ z_- \bar{\rho}$. However, this parameter is not sufficient, as z_{is} is the same for a 2:2 or a 4:1 electrolyte and it is the second coefficient z_{as} which is really characteristic of the asymmetry in valence between ions. With these notations we have

$$\beta \delta H = -\frac{\bar{\rho}}{2z_{\text{is}}^2} \int [\delta s(\mathbf{r}) - \delta s^2(\mathbf{r})] \delta q^2(\mathbf{r}) d\mathbf{r} - \frac{z_{\text{as}} \bar{\rho}}{3! z_{\text{is}}^3} \int [1 - 2\delta s(\mathbf{r}) + 3\delta s^2(\mathbf{r})] \delta q^3(\mathbf{r}) d\mathbf{r} + \frac{2\bar{\rho}}{4! z_{\text{is}}^4} \int (1 + z_{\text{as}}^2) [1 - 3\delta s(\mathbf{r}) + 6\delta s^2(\mathbf{r})] \delta q^4(\mathbf{r}) d\mathbf{r} + \dots \quad (6)$$

Note that the quadratic term in the Hamiltonian remains diagonal for the q and s fields also for the valence asymmetric systems and odd terms in q appear only in $\beta \delta H$, the smallest odd power in q being 3.

As in ref 20, the Hamiltonian can be further simplified by scaling the charge density field $\delta q \rightarrow \delta Q = \delta q/z_{\text{is}}$ and by defining a new unit charge $\tilde{e} = z_{\text{is}}e$. In this case for the even terms we recover the expansion of the symmetric 1:1 electrolyte and supplementary terms dependent on z_{as} . The Hamiltonian is

$$\beta H = \bar{\rho}V + \frac{\bar{\rho}}{2} \int [\delta s^2(\mathbf{r}) + \delta Q^2(\mathbf{r})] d\mathbf{r} + \beta \delta H + \beta H^{\text{Coul}}[Q(\mathbf{r})] \quad (7)$$

with

$$\beta \delta H = -\frac{\bar{\rho}}{2} \int \delta s(\mathbf{r}) \delta Q^2(\mathbf{r}) d\mathbf{r} + \frac{\bar{\rho}}{12} \int \delta Q^4(\mathbf{r}) d\mathbf{r} - \frac{\bar{\rho} z_{\text{as}}}{6} \int \delta Q^3(\mathbf{r}) d\mathbf{r} + \frac{\bar{\rho} z_{\text{as}}^2}{12} \int \delta Q^4(\mathbf{r}) d\mathbf{r} + \dots \quad (8)$$

where we have kept from eq 6, for clarity, only the terms of interest. The Coulomb interaction term is also modified

$$\beta H^{\text{Coul}}[q] = \frac{K_D^2}{8\pi\bar{\rho}} \int \frac{\delta Q(\mathbf{r}) \delta Q(\mathbf{r}')}{|\mathbf{r} - \mathbf{r}'|} d\mathbf{r} d\mathbf{r}' \quad (9)$$

where we have introduced the inverse Debye length, $K_D = (\beta(z_+^2 \bar{\rho}_+ + z_-^2 \bar{\rho}_-)e^2/\epsilon)^{1/2} = (\beta \bar{\rho} \tilde{e}^2/\epsilon)^{1/2}$, which shows that K_D has the same expression as for the 1:1 electrolyte except that the elementary charge is now \tilde{e} . Note that the scaling introduced in this section can be considered as a simple renormalization of the electrostatic quantities in relation with the ionic strength. In the following, we perform all calculations in terms of the charge density field δQ and transform the result in the physical field δq at the end of the calculations.

The parameter z_{is} has been completely absorbed in the new field δQ and the charge \tilde{e} and as in ref 20 we can use the results for the 1:1 symmetric electrolyte and we mainly need to focus on the new terms in comparison to the symmetric case, associated with the asymmetry parameter z_{as} . For the interfacial properties, at the one loop level of the calculations we will assimilate the activity $\bar{\rho}$ and the average density ρ .

III. Charge Profile at the PZC

The calculation of the charge profile illustrates the peculiarity of the asymmetric systems. For the symmetric $z_+ z_-$ electrolytes at the neutral interface, for reasons of symmetry, average quantities which include an odd number of charge densities, as for instance the charge profile, vanish. Another way of stating this is by noting that it is impossible by applying the Wick

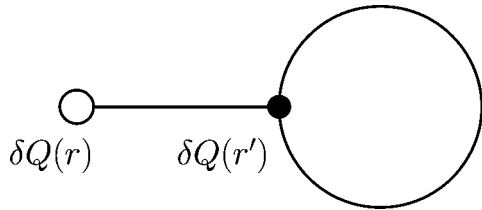


Figure 1. Diagram for the calculation of the charge density profile as described in the text.

theorem to pair the charge fields and simultaneously calculate a quantity with an odd number of charge fields, because this would imply the existence of odd coupling constants. Such odd terms exist for the asymmetric systems as a consequence of the expansion of the entropic contribution to the Hamiltonian. The first contribution is due to the three-body coupling in eq 8 and corresponds to the diagram in Figure 1 where we have the standard 1/2 symmetry coefficient associated and the analytic expression is

$$\langle \delta Q(\mathbf{r}) \rangle = \frac{\rho z_{\text{as}}}{2} \int d\mathbf{r}' \langle \delta Q(\mathbf{r}) \delta Q(\mathbf{r}') \rangle \delta Q(\mathbf{r}') \delta Q(\mathbf{r}') \quad (10)$$

where the inhomogeneous correlation functions are those given in ref 20 where

$$\langle \delta Q(\mathbf{r}) \delta Q(\mathbf{r}') \rangle = \frac{1}{\rho} \left[\delta(\mathbf{r} - \mathbf{r}') - \frac{K_D^2}{4\pi} \frac{e^{-K_D |\mathbf{r} - \mathbf{r}'|}}{|\mathbf{r} - \mathbf{r}'|} + \int \frac{d\mathbf{K}}{(2\pi)^2} e^{-i\mathbf{K}(\mathbf{R} - \mathbf{R}') - K'(x+x')} \frac{K_D^2 (K - K')}{2K'(K + K')} \right] \quad (11)$$

where x and x' are distances of the points from the wall and \mathbf{R} and \mathbf{R}' are respectively the projections of \mathbf{r} and \mathbf{r}' parallel to the wall and where $K' = \sqrt{(K^2 + K_D^2)^{1/2}}$. In the previous correlation, when calculated at the same point, we renormalize the dirac distribution as indicated in ref 17. The bulk part which does not depend on the distance to the wall vanishes with the rest of the graph as a consequence of the electroneutrality condition $\int \langle \delta Q(\mathbf{r}) \delta Q(\mathbf{r}') \rangle d\mathbf{r}' = 0$. Finally, the excess contribution at the wall gives²¹

$$\langle \delta Q(\mathbf{r}) \delta Q(\mathbf{r}) \rangle = \frac{K_D^3}{4\pi\rho} I(\hat{x}) \quad (12)$$

where we used the reduced distance to the wall $\hat{x} = xK_D$ and $I(\hat{x}) = \int_1^\infty e^{-2\hat{t}} / (t + \sqrt{t^2 - 1})^2 dt$.

We finally obtain our result, the profile for the charge

$$q(\hat{x}) = \frac{1}{2} z_{\text{as}} z_{\text{is}} \rho \eta F(\hat{x}) \quad (13)$$

where the coefficient $\eta = K_D^3 / (8\pi\rho)$ and the function $F(x) = -2I(x) + f(x) + c_0 e^{-x}$ where

$$f(\hat{x}) = \int_1^\infty \left[\frac{e^{-\hat{x}}}{(2t-1)} - 2 \frac{e^{-2\hat{t}}}{(2t-1)(2t+1)} \right] \frac{dt}{(t + \sqrt{t^2 - 1})^2} \quad (14)$$

and $c_0 = -\pi\sqrt{3}/12 + \ln 3/4 + 1/4 \approx 0.071203$.

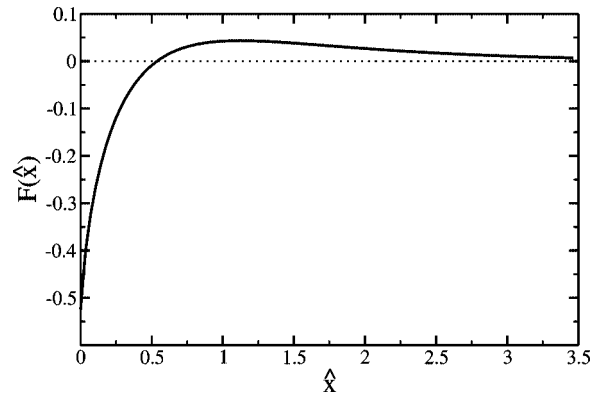


Figure 2. F function, proportional to the charge density profile, as a function of the distance to the wall in reduced units.

The generic form of the function $F(x)$ is given in Figure 2. At the wall, we have $F(0) = -2/3 + 2c_0$, and thus the charge density at contact is

$$q(0) = z_{\text{as}} z_{\text{is}} \rho \eta \left(c_0 - \frac{1}{3} \right) \quad (15)$$

We also note that the integral of F is zero, implying that as expected the profile verifies the electroneutrality condition $\int q(x) dx = 0$.

IV. Potential Profile at the PZC

The electric potential can be obtained using the charge profile from the exact expression

$$\beta e \psi(x) = -\frac{\beta e^2}{\epsilon} \int_x^\infty (x' - x) q(x') dx' \quad (16)$$

using equation (13), we obtain

$$\beta e \psi(x) = -\frac{z_{\text{as}} \eta}{z_{\text{is}} 2} \int_{\hat{x}}^\infty (\hat{x}' - \hat{x}) F(\hat{x}') d\hat{x}' \quad (17)$$

$$= \frac{z_{\text{as}}}{z_{\text{is}}} \eta G(\hat{x}) \quad (18)$$

where

$$G(\hat{x}) = \int_1^\infty \frac{e^{-2\hat{t}} dt}{(2t^2 + 2t\sqrt{t^2 - 1} - 1)(4t^2 - 1)} - c_1 e^{-\hat{x}} \quad (19)$$

with $c_1 = \pi\sqrt{3}/24 + \ln 3/8 - 1/4 \approx 0.11405$. The generic form of the function $G(x)$ is given in Figure 3. We note that the derivative of this electric potential, which is proportional to the electric field, is zero at the interface as expected for a neutral hard wall. At the contact with the wall, we have

$$\beta e \psi(0) = -\frac{z_{\text{as}}}{z_{\text{is}}} \eta c_0 \quad (20)$$

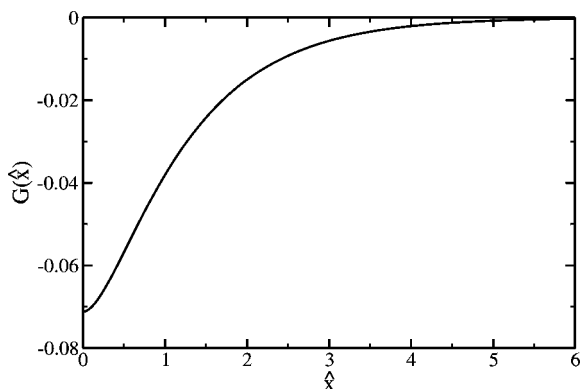


Figure 3. G function, proportional to the electric potential profile, as a function of the distance to the wall in reduced units.

V. Charge Contact Theorem

In ref 16, we have derived the charge contact theorem which relates the contact value of the charge profile to the electric field across the interface. Using this exact relation, in the following, we verify the consistency of our expressions for the charge density and for the electric potential profiles. For an asymmetric in valence system of point ions, the charge contact theorem reads

$$q(0) = \beta e \int_0^\infty (z_+^2 \rho_+(x) + z_-^2 \rho_-(x)) \left(\frac{\partial \psi(x)}{\partial x} \right) dx + \beta(z_+ P_+ + z_- P_-) \quad (21)$$

Note that in comparison to the notations in ref 16, here q is a density and does not include the electric charge. At the lowest order in the loop expansion, we can take the profile of the density and the electric potential respectively at the zero loop order which corresponds to a constant profile and at the first order, which is our result eq 18. So the first term becomes

$$-\beta e z_{\text{is}}^2 \rho \psi(0) = (z_+ - z_-) \rho \eta c_0 = z_{\text{as}} z_{\text{is}} \rho \eta c_0 \quad (22)$$

For the second term, at the same order, the partial pressures are given by the Debye approximation

$$\beta P_\pm = \frac{z_\pm \beta P}{z_+ + z_-} \quad (23)$$

where $\beta P = -K_D^3/(24\pi) = -\rho\eta/3$ is the total pressure. We thus have

$$\beta(z_+ P_+ + z_- P_-) = \beta(z_+ - z_-) P \quad (24)$$

$$= -\frac{1}{3} z_{\text{as}} z_{\text{is}} \eta \rho \quad (25)$$

We can see that the sum of the two contributions eqs 22 and 25 gives the value obtained from the direct calculation of the charge density profile given in eq 15. This shows the consistency of our results for the charge density and electric potential profiles obtained at the first order in the loop expansion with the exact contact charge relation.

VI. Discussion

In sections III and IV, we have shown the existence of a spontaneous polarization of a neutral interface. This phenomenon is absent in symmetric systems where we have the same number of anions and cations at each point across the neutral interface, although we have shown there is a profile for the total number of ions.¹⁹ The polarization is then directly related to the asymmetry in valence of the ions, that is, to the displacement of the equilibrium in the number of the ionic species in order to satisfy the electroneutrality condition. A way of understanding this profile is to consider the depletion of the ionic profiles due to the electrostatics existing at interfaces.¹⁹ In the usual electrochemical language this phenomenon can be rationalized as the cost of rupturing the ion atmosphere near the surface. Naturally, for a more highly charged ion we will have two effects, and the ion cloud will be even more difficult to disrupt and also less extended. Assuming $z_+ > z_-$, going from the bulk toward the interface, the less charged anions which have a more extended ion atmosphere will be to see the interface and their density will start decreasing moving toward the wall. In this region, the charge will be positive. Getting closer to the wall, the more highly charged cations will start being affected and their density will then also decrease. This depletion effect will be strong as their ionic atmosphere is more tightly bound. In this region, the charge will start being negative. Thus, we have a negative charge profile at contact, which is followed by a distribution of negative charge which is then electrically compensated by positive region further away from the wall. Such qualitative statements have been discussed on the occasion of the contact theorem for asymmetric electrolytes.²² These effects will diminish with increasing temperature as one would expect of an energetically controlled phenomenon. The phenomenon is a balance between the electrostatics and the thermal agitation and this balance controls the ionic atmosphere distribution. From our field theoretical approach, the effect is a balance between the entropic functional term and the Coulomb term in the Hamiltonian. This is consistent as the entropic functional term is essentially related with the temperature energy scale. However, in the field theory formalism we emphasize not only the thermal agitation but also on the combinatorics coming from the two entropic functionals related to the two ionic species, which quantify the thermal disorder.

More quantitatively, we have seen in section V that the profiles are such that they verify consistently the charge contact theorem at a given order of approximation. From eqs 13 and 18, the expressions of the charge density and of the electric potential profiles are analytic and simple. Here are some of their characteristic features. The two profiles depend respectively on the universal functions F and G in terms of the reduced distance x and linearly on the loop expansion parameter η . As a consequence, we can see that similar to the desorption phenomenon and to the anomalous capacitance behavior²⁰ this polarization of the interface increases as the reduced temperature decreases. We recall that the reduced temperature is proportional to the temperature and to the dielectric constant and inversely proportional to the product of the ionic charges. Therefore, there is a fair number of physical systems which correspond to a low reduced temperature as it is possible to decrease the systems' temperature or dielectric constant or conversely consider highly charged ionic species. Typically for a 0.05 molar solution of a 2:1 electrolyte at room temperature in water we have $\eta \approx 0.909$. Then, the value of the profiles are linear on the product $z_{\text{as}} z_{\text{is}} = z_+ - z_-$ for the charge profile where as the reduced electric potential scales on the ratio $z_{\text{as}}/z_{\text{is}} = (z_+ - z_-)/(z_+ z_-)$. As a

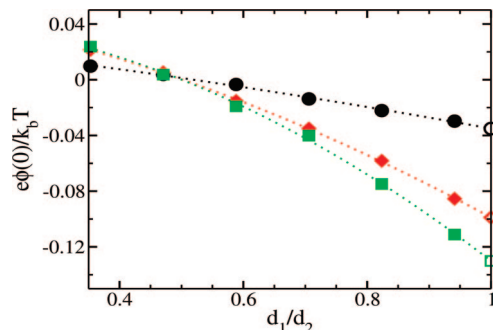


Figure 4. PZC data from ref 15 (circles, diamonds, and squares) for the size asymmetric 2:1 electrolytes for concentrations 0.05, 0.5, and 1.0 mol/L, respectively, extrapolated to the equal diameter systems (empty symbols). The dotted lines are the LLSQ fit used.

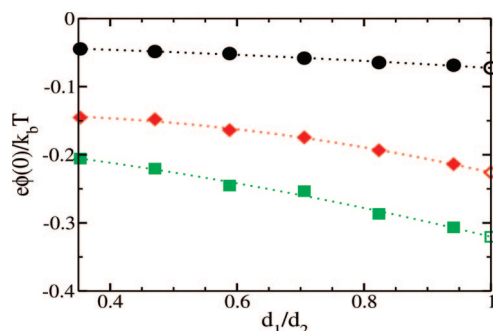


Figure 5. Same as in Figure 4 for the 3:1 electrolyte and concentrations 0.033, 0.333, and 1.0 mol/L.

TABLE 1: Extrapolation of the PZC by LLSQ Fit for the 2:1 Electrolyte from Numerical Data Results in Ref 15

concentration	η	PZC sim	PZC FT
0.05 mol/L	0.909	-0.0351	-0.0321
0.5 mol/L	2.87	-0.0989	-0.101
1.0 mol/L	4.07	-0.130	-0.143

TABLE 2: Extrapolation of the PZC by LLSQ Fit for the 3:1 Electrolyte from Numerical Data Results in Ref 15

concentration	η	PZC sim	PZC FT
0.033 mol/L	1.57	-0.0726	-0.0736
0.333 mol/L	4.98	-0.226	-0.234
0.666 mol/L	7.04	-0.320	0.331

consequence, the behaviors of the charge and of the electric potential are different. The charge scales proportionally to the difference $z_+ - z_-$, whereas the ratio z_{as}/z_{is} is bound by 1 for high charge asymmetries.

We have compared quantitatively our point ion expression for the PZC with the numerical simulation results in ref 15. Note that for this comparison, the contact value distance corresponds to half the ionic diameter for the finite-sized ions of the MC simulations, whereas for the point ions it corresponds to a vanishing distance to the wall. As the size asymmetry is immaterial for the point ions, we first extrapolate the simulation results for the equal size ions using a linear least-squares quadratic (LLSQ) fit for the 2:1 and 3:1 electrolytes as shown in Figures 4 and 5. The fits give for the various concentrations used in ref 15 the PZCs shown in Tables 1 and 2 in the column PZCsim, where we have also given the value of the parameter η . For all these systems we note that $\eta \geq 1$, which indicates that beyond mean field correlations are important. In contrast to the numerical simulation results, simple, analytic approaches of the liquid state theory like the LMGC (linear modified

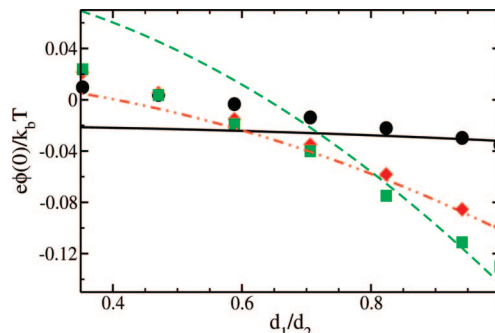


Figure 6. PZC as a function of the diameter ratio, for a 2:1 electrolyte and the same physical parameters, temperature, and dielectric constant as in ref 15. The symbols (circles, diamonds, and squares) are for the numerical simulations data and the empty symbol for the extrapolated value for equal diameters, and the curves (full, dotted-dashed, and dashed) are for the field theory plus the LMGC theory¹⁵ presented in the order of the concentrations 0.05, 0.5, and 1.0 mol/L.

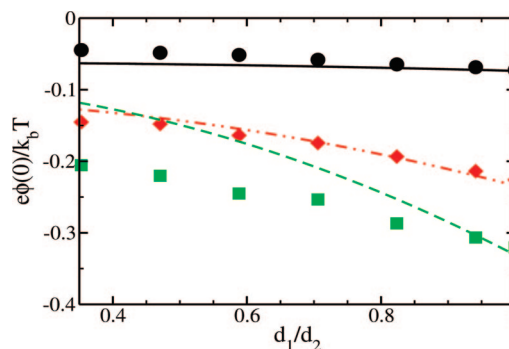


Figure 7. PZC as a function of the diameter ratio, for a 3:1 electrolyte and the same physical parameters temperature, dielectric constant as in ref 15. The meanings of the symbols and curves are those of Figure 6 except that the concentrations are 0.033, 0.333, and 1.0 mol/L.

Gouy–Chapman) and MSA (mean spherical approximation) theory give a vanishing value of the PZC.¹⁵

The PZC obtained from the field theory is given in the last column of Tables 1 and 2. For nearly all values, the results of the field theory for the simple point ions are very close to those of the simulations, for the concentrations investigated and for both 2:1 and 3:1 electrolytes. The only point which is not as accurate corresponds to the highest density considered for the 2:1 electrolyte. The overall agreement of the theory seems to indicate that the excluded volume effects are not crucial. This favors our interpretation that this polarization phenomenon is a balance between the entropic and the interaction functionals in the Hamiltonian. The presence of the entropic term implies that the phenomenon is related to the number balance of the ionic species, which follows the valence asymmetry.

Given the results of the simple point ion model, we have considered extending the comparison for non symmetric electrolyte both in size and in valence as they are studied in ref 15. In this article, for valence symmetric systems the LMGC and MSA approaches give a reasonable dependence with respect to the ionic diameter ratio. It is then tempting to assume an additive approximation combining the size asymmetry well described by standard liquid state theory approaches and the valence asymmetry which is well described by our field theory approach. We have used this assumption for the results presented in Figures 6–9.

In Figures 6 and 7, the theory is obtained by adding the PZC values of the LMGC approach to those of the field theory (Tables 1 and 2), respectively, for the 2:1 and 3:1 electrolytes

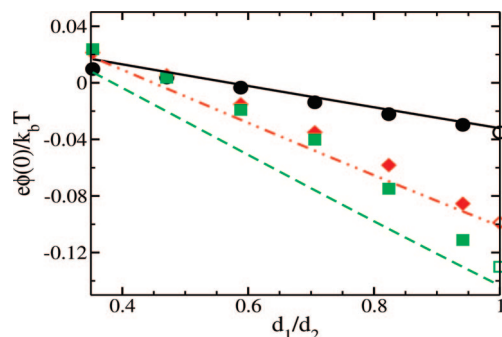


Figure 8. PZC as a function of the diameter ratio, for a 2:1 electrolyte, with caption identical to that in Figure 6 except that the MSA approximation is used in place of the LMGC approximation.

and for the corresponding concentrations. For both types of electrolytes, this approximation gives good results for near symmetric in size systems. At the intermediate density considered, the agreement extends over all diameter ratios whereas it respectively underestimates and overestimates the effect at low and high densities.

In Figures 8 and 9, we replace the PZC values of the LMGC by those of the MSA approach. In this case, the results are overall much closer to the simulation results for both type of valences and all concentrations. However, in the case of the 2:1 electrolyte the approximation is more successful at lower concentration. Whereas for the 3:1 electrolyte, the comparison is incredibly good over the whole concentration range considered.

Thus, simply adding the PZC effects due to the size and valence asymmetries gives rather good results and allows with a simple model the simultaneous description of both asymmetries. We believe that the discrepancy appears to be lower for the 3:1 electrolyte as in this case the valence effect which is rather well predicted by the field theory is larger and possibly may partly hide the discrepancies in the description of the size effects.

Finally, we consider the comparison with computer simulation for the charge density and the electrical potential profiles. The theoretical results are given by eqs 13 and 18 correspondingly. Unfortunately, the computer data for charge and potential profiles for size symmetrical electrolytes, at a neutral interface, are known only from ref 14 for the 2:1 electrolyte at 0.5 mol/L which is not the best choice for such comparison. As we can see from Table 1, at these conditions the theory gives for the PZC -0.101 while from the extrapolated simulation¹⁵ we have -0.0989 . Moreover, at these conditions, the computer simulation from ref 14 gives -0.0892 . The comparison of the theoretical and computer results for the charge density and the electrical potential profiles is presented in Figures 10 and 11, respectively, where the distance of closest approach which is zero for point ions and 0.5 in diameter units for hard spheres are set to be the same distance from the wall. As we can see, for the electrical potential the agreement between theory and computer simulation data is quite good. However, for the charge density profile we have only a qualitative agreement. The better agreement for the electrical potential can be related to the fact that its expression corresponds to a moment of the charge density profile with respect to the distance from the wall. In Figure 10, it can be seen that the theory reproduces more accurately the charge profile further away from the interface, namely the contribution from the profile which has a stronger weight in the electrical potential expression. For the contribution of the charge density profile closer to the interface there can be a compensation as the theory is according to the distance both, once larger and once smaller than the computer simulation data.

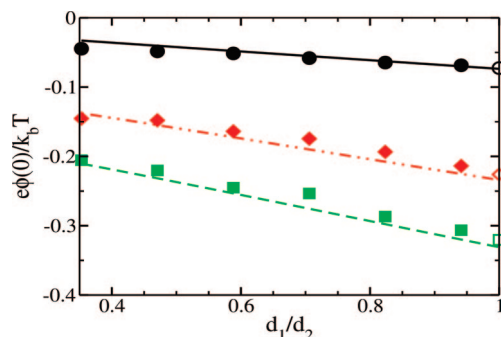


Figure 9. PZC as a function of the diameter ratio, for a 3:1 electrolyte, with caption identical to that in Figure 7 except that the MSA approximation is used in place of the LMGC approximation.

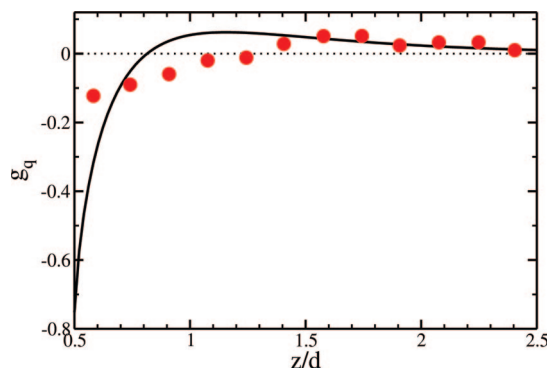


Figure 10. Normalized charge density profile g_q (charge density divided by the total bulk concentration of ions), for a 2:1 electrolyte at 0.5 mol/L where the line is the present theory eq 13 and the points the numerical simulation results.¹⁴

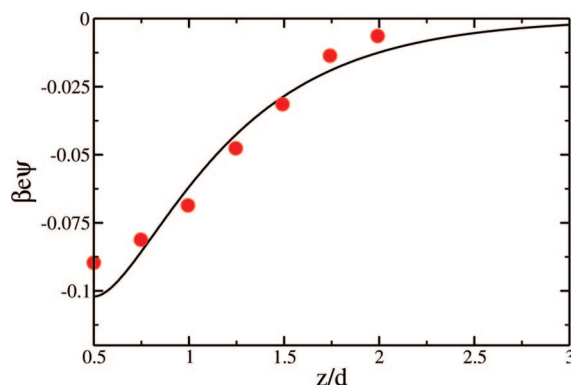


Figure 11. Electric potential for a 2:1 electrolyte at 0.5 mol/L where the line is the present theory eq 18 and the points the numerical simulation results.¹⁴

VII. Conclusion

In this paper, we have studied the behavior of valence asymmetric electrolytes at simple hard neutral interfaces. We have discussed the existence of a polarization of the neutral interface for these systems which is not related to any specific interaction with the interface.

Using the field theoretical approach for a point ion model, we illustrate the connection between this phenomenon and the entropic functional term in the Hamiltonian. More precisely, we show that the effect is not related to any volume exclusion potential but rather it is connected to the number balance between the ions. This phenomenon is quite fundamental as its origin comes from the combinatorics and counting of the states in the phase space set by basic rules of the quantum mechanics. These familiar rules exist even in the wholly classical description

of systems. They give the entropic contribution of the particles of the same kind which are indistinguishable and as a consequence also set the combinatory for anions and cations which are discernible species. The physics of these rules appears in the entropic part of the functional of our field theory Hamiltonian. The role of this entropy has previously been emphasized discussing the desorption phenomenon and the related anomalous capacitance behavior. In this case, the entropic functional leads to a coupling between charge and total density fields.^{11,23} In the present work, the same entropic functional gives couplings for the charge field alone and gives the correction to the trivial vanishing mean field charge density profile. Another interesting aspect, in the approach, is that on the field variables we are allowed algebraic operations (e.g., linear combinations of the fields like the charge or the total density) which turn out to be meaningful physically and are less straightforward to implement when discussing particles. Finally, for the charge and the electric potential profile, we obtain expressions which are analytic and rather simple with well-identified scaling behaviors in terms of the physical parameters. In particular, we discuss the role of two parameters related to multivalency. One is the product of the valences, which is related to the ionic strength in the system. The second is more characteristic of the asymmetry as it is proportional to the difference of the valences.

We believe that this study illustrates the interest of our FT approach. One important aspect is the original description of the quantum mechanical degrees of freedom which leads to new interpretations and allows for certain systems to obtain a clear physical picture and simple application in comparison to other approaches.

Acknowledgment. M.H. and D.d.C. are grateful to J. P. Badiali for enlightening discussions and for the support of the National Academy of Science of Ukraine (NASU) and the CNRS, in the framework of project no. 21303. The authors are also grateful to M. Valiskó, D. Boda, and D. Henderson for providing their simulation data results.¹⁵

References and Notes

- (1) Kilic, M. S.; Bazant, M. Z.; Ajdari, A. *Phys. Rev. E* **2007**, *75*, 021502; *Ibid* 021503.
- (2) Kornyshev, A. A. *J. Phys. Chem. B* **2007**, *111*, 5545.
- (3) Boda, D.; Henderson, D.; Chan, K. Y. *J. Chem. Phys.* **1999**, *110*, 5346.
- (4) Boda, D.; Henderson, D.; Chan, K. Y.; Wasan, D. T. *Chem. Phys. Lett.* **1999**, *308*, 473.
- (5) Mier-y-Teran, L.; Boda, D.; Henderson, D.; Quinones-Cisneros, S. E. *Mol. Phys.* **2001**, *99*, 1323.
- (6) Holovko, M.; Kapko, V.; Henderson, D.; Boda, D. *Chem. Phys. Lett.* **2001**, *341*, 363.
- (7) Pizio, O.; Patrykiewicz, A.; Sokołowski, S. *J. Chem. Phys.* **2004**, *121*, 11957.
- (8) Reszko-Zygmunt, J.; Sokołowski, S.; Henderson, D.; Boda, D. *J. Chem. Phys.* **2005**, *122*, 084504.
- (9) Bhuiyan, L. B.; Outhwaite, C. W.; Henderson, D. *J. Chem. Phys.* **2005**, *123*, 034704.
- (10) Henderson, D.; Boda, D. *J. Electroanal. Chem.* **2005**, *582*, 16.
- (11) di Caprio, D.; Stafiej, J.; Borkowska, Z. *J. Electroanal. Chem.* **2005**, *582*, 41.
- (12) Valiskó, M.; Henderson, D.; Boda, D. *J. Mol. Liq.* **2007**, *131*, 179.
- (13) Bhuiyan, L. B.; Outhwaite, C. W.; Henderson, D. *Langmuir* **2006**, *22*, 10630.
- (14) Torrie, G. M.; Valleau, J. P.; Outhwaite, C. W. *J. Chem. Phys.* **1984**, *81*, 6296.
- (15) Valiskó, M.; Henderson, D.; Boda, D. *J. Phys. Chem. B* **2004**, *108*, 16548.
- (16) Holovko, M.; di Caprio, D.; Badiali, J. P. *J. Chem. Phys.* **2005**, *123*, 234705. Holovko, M.; di Caprio, D.; Badiali, J. P. *J. Chem. Phys.* **2007**, *127*, 014106. Holovko, M.; di Caprio, D.; Badiali, J. P. *J. Chem. Phys.* **2008**, *128*, 117102.
- (17) di Caprio, D.; Badiali, J. P. *J. Phys. A: MathGen* **2008**, *41*, 125401.
- (18) di Caprio, D.; Badiali, J. P.; Holovko, M. *J. Phys. A: MathGen* **2008**, In press.
- (19) di Caprio, D.; Stafiej, J.; Badiali, J. P. *Electrochim. Acta* **2003**, *48*, 2967.
- (20) di Caprio, D.; Valiskó, M.; Holovko, M.; Boda, D. *Mol. Phys.* **2006**, *104*, 3777.
- (21) di Caprio, D.; Stafiej, J.; Badiali, J. P. *Mol. Phys.* **2003**, *101*, 2545.
- (22) Holovko, M.; di Caprio, D. *J. Chem. Phys.* **2008**, *128*, 174702.
- (23) di Caprio, D.; Valiskó, M.; Holovko, M.; Boda, D. *J. Phys. Chem. C* **2007**, *111*, 15700.

JP8086573